DOI: 10.1002/ejoc.201500139

A DFT Study of Inter- and Intramolecular Aryne Ene Reactions

Patricia Pérez*[a] and Luis R. Domingo*[b]

Keywords: Reaction mechanisms / Density functional theory / Ene reaction / Arynes

The molecular mechanisms of inter- and intramolecular aryne-ene reactions have been theoretically studied by DFT methods at the MPWB1K/6-311G(d,p) level. These reactions proceed through a one-step mechanism via nearly asynchronous transition states (TSs), in which the C–C single bond formation is slightly more advanced than the hydrogen transfer process. These ene reactions show very low activation enthalpies (<1 kcal/mol) and are strongly exothermic by more than 73 kcal/mol. An electron localisation function (ELF) topological analysis of the changes of electron density during these ene reactions indicates that the bonding changes are nonconcerted. ELF topological analysis of the electron density in the C1–C2 bonding region of benzyne indicates that the 1,2-pseudodiradical vinyl structure, rather than a structure with a C≡C triple bond, is responsible for the very high reactivity of these species.

Introduction

One of the simplest ways to achieve a C–C bond formation is through the ene reaction, which involves the reaction of an alkene with an allylic C–H bond, named the ene component, and an ethylene, named the enophile.[1] In the simplest ene reaction, propene (**1**) reacts thermally with the C=C double bond of ethylene (**2**) to form a new C–C single bond together with the migration of the allylic hydrogen atom and the propene C=C double bond to yield 1-pentene (**3**, see Scheme 1).

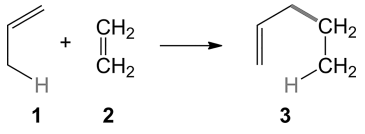

Scheme 1. The ene reaction.

Although ene reactions between propene and alkenes are feasible, the high activation energies associated with these reactions make them experimentally impracticable. Thus, to experimentally perform the ene reaction, the enophile should be electrophilically activated.

Arynes are highly reactive intermediates[2] and have been comprehensively utilised as building block in organic synthesis.[3] However, the rigorous reaction conditions required for their preparation have greatly limited their applications. With the emergence of moderate preparation methods for arynes, they have attracted considerable attention for synthetic applications.[4]

Although many ene reactions have been reported, there are few examples of aryne-ene (AE) reactions. Recently, Lautens et al. reported the intramolecular aryne-ene (intra-AE) reaction as a straightforward route to benzofused carbo- and heterocycles (see Scheme 2).[5] The reactions were performed under mild conditions, that is, 24 h at room temperature. This intramolecular strategy allowed the corresponding benzofused carbo- and heterocycles to be obtained with a high level of chemo-, regio- and stereoselectivity.[5]

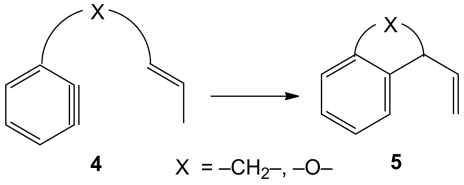

Scheme 2. The intramolecular ene reaction studied by Lautens et al.[5]

More recently, Yin et al.[6] studied the intermolecular ene reactions (inter-AE) of arynes with olefins (see Scheme 3).

A wide range of alkenes were used, and the ene adducts were obtained in good yields (80% for **8** and 75% for **10** and **12**) under mild conditions, that is, 12 h at 25 °C.[6]

Intra-AE reactions were computationally studied at the B3LYP/6-31G(d) level by Lautens et al.[5] For the intra-AE reaction of **13** (see Scheme 4), the authors proposed an earlier pseudochairlike transition state (TS) in a concerted process. However, bond formation was asynchronous, and the C–C bond formation was more advanced. The activation energy for this process was computed to be 4.5 kcal/mol, in clear agreement with the mild reaction conditions.[5]

[a] Facultad de Ciencias Exactas, Departamento de Ciencias Químicas, Laboratorio de Química Teórica, Universidad Andres Bello,
Av. República 230, 8370146 Santiago, Chile
E-mail: p.perez@unab.cl
http://www.unab.cl
[b] Departamento de Química Orgánica, Universidad de Valencia, Dr. Moliner 50, 46100 Burjassot, Valencia, Spain
http://www.luisrdomingo.com

Supporting information for this article is available on the WWW under http://dx.doi.org/10.1002/ejoc.201500139.

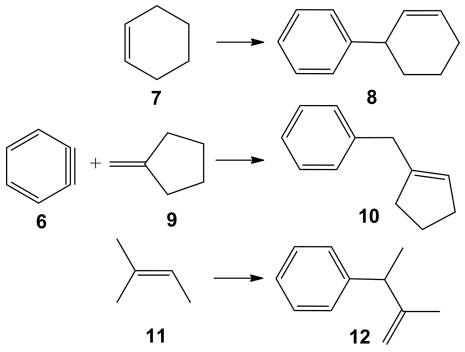

Scheme 3. Intermolecular ene reactions studied by Yin et al.[6]

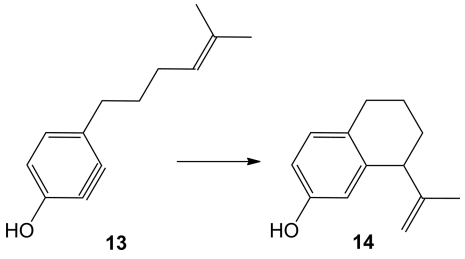

Scheme 4.

The stereochemistry in the intra-AE reactions was analysed for the reaction of the model substrate **15**, which has an allylic stereocentre.[5] The TSs in which the allylic methyl substituent was placed in a pseudoequatorial position were considered. Rotation about the single C–C bond provided two stereoisomeric TSs (see Scheme 5). The 1,3-allylic strain in TS**15**-b raises its energy 4.2 kcal/mol above that of TS**15**-a; this result is in clear agreement with the experimental outcome, in which the ene cycloadduct showed a *trans* stereochemistry.

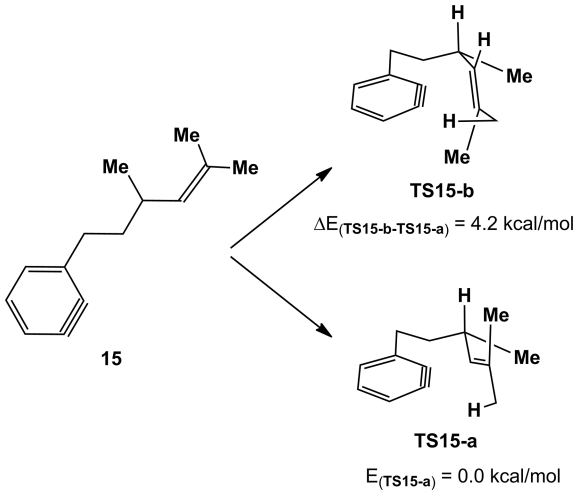

Scheme 5.

The mechanism of the ene reactions of isobutene (**16**) with twelve enophiles of increasing electrophilicity has been very recently studied.[7] The activation energies range from 34.7 kcal/mol for the most unfavourable ene reaction with ethylene (**2**) to –1.2 kcal/mol for the most favourable ene reaction with the BF_3–formaldehyde complex **18** (see Scheme 6). As in Diels–Alder (DA) reactions,[8] a very good correlation between the activation energy and the global electron density transfer (GEDT) at the corresponding TS was found. Thus, the polar ene (P-ene) reaction mechanism was proposed;[7] for this mechanism, the more polar the ene is, the faster the reaction is. For these twelve ene reactions, the ene reaction with **2** presented the highest activation energy of 34.7 kcal/mol and the lowest GEDT of 0.13 e; therefore, this reaction was classified as a nonpolar ene (N-ene) reaction.

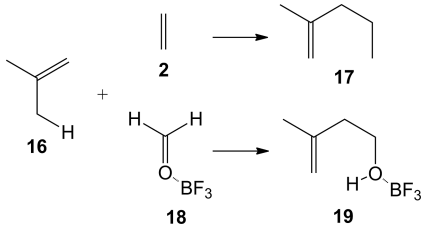

Scheme 6.

All of these studied reactions presented one-step mechanisms via highly asynchronous TSs in which the C–C bond formation is very advanced and the hydrogen transfer is very delayed.[7] An electron localisation function[9] (ELF) topological analysis of the bonding changes along these ene reactions indicated that most of the P-ene reactions proceeded through a nonconcerted two-stage one-step mechanism.[10] In this mechanism, the hydrogen transfer process, which occurs in the second stage of the reaction, does not begin until the complete formation of the new C–C single bond, which is completed in the first stage of the reaction.[7]

Herein, mechanistic studies of the inter-AE reactions of benzyne (**6**) with cyclohexene (**7**), methylenecyclopentane (**9**), and 2-methyl-2-butene (**11**), which were performed experimentally by Yin[6] (see Scheme 3), and the intra-AE reaction of aryne **13** studied by Lautens[5] (see Scheme 4) are performed to understand the behaviour of arynes as the enophile components in ene reactions. ELF topological analyses of the C–C bond formation and the hydrogen transfer process in both inter- and intra-AE reactions were performed to establish the molecular mechanisms of these AE reactions.

Computational Methods

All stationary points involved in these aryne-ene reactions were first optimised by using the B3LYP[11] exchange-correlation functional together with the standard 6-31G(d) basis set.[12] Then, the gas-phase geometries were reoptimised by using the MPWB1K[13] exchange-correlation functional, which gives good results for thermochemistry, thermochemical kinetics, hydrogen bonding and weak interactions, together with the standard 6-311G(d,p) basis set.[12] The optimisations were performed by the Berny analytical gradient optimisation method.[14] The stationary points were characterised by frequency computations to verify that

the TSs had only one imaginary frequency. The intrinsic reaction coordinate (IRC) paths[15] were traced to check the energy profiles connecting each TS to the two associated minima of the proposed mechanism by the second-order González–Schlegel integration method.[16] All studied ene reactions presented a one-step mechanism. The IRC analyses of the corresponding TSs directly connected them with the reagents and aryne–ene adducts. As arynes have a pseudodiradical character, the stability of the closed-shell wave functions of the arynes and the corresponding TSs were checked with the Stable = opt keyword. The wave functions of all species were stable under the perturbations considered; thus, more stable open-shell solutions were discarded. The solvent effects of acetonitrile for the inter-AE reactions and tetrahydrofuran (THF) for the intra-AE reaction were taken into account by full optimisation of the gas-phase structures at the MPWB1K/6-311G(d,p) level by using the polarisable continuum model (PCM) as developed by the Tomasi group[17] in the framework of the self-consistent reaction field (SCRF).[18] The integral equation formalism variant (IEFPCM) is the SCRF method used in this work. The electronic structures of stationary points were analysed by the natural bond orbital (NBO) method[19] and by ELF topological analysis, $\eta(r)$.[20] The ELF study was performed with the TopMod program[21] with the corresponding MPWB1K/6-311G(d,p) monodeterminantal wave functions of the selected structures of the IRC. All computations were performed with the Gaussian 09 suite of programs.[22]

The global electrophilicity index, ω, is given by the expression $\omega = (\mu^2/2\eta)$, in terms of the electronic chemical potential μ and the chemical hardness η.[23] Both quantities may be approached in terms of the one-electron energies of the frontier molecular orbitals, that is, the highest occupied molecular orbital (HOMO) and lowest unoccupied molecular orbital (LUMO), ε_H and ε_L, as $\mu = (\varepsilon_H + \varepsilon_L)/2$ and $\eta = (\varepsilon_L - \varepsilon_H)$, respectively.[24] The empirical (relative) nucleophilicity index[25] N is based on the HOMO energies obtained within the Kohn–Sham scheme[26] and is defined as $N = E_{HOMO}(Nu) - E_{HOMO}(TCE)$; tetracyanoethylene (TCE) is the reference because it presents the lowest HOMO energy in a long series of molecules already investigated in the context of polar organic reactions. This choice produces a convenient nucleophilicity scale with positive values.

Results and Discussions

The present study has been divided into three parts: (1) Firstly, the inter-AE reactions of benzyne (**6**) with alkenes **7**, **9** and **11** as well as the intra-AE reaction of aryne **13** were studied. (2) In the second part, ELF topological analyses of the inter-AE reaction of **6** with **16** and the intra-AE reaction of aryne **13** were performed. (3) Finally, the DFT reactivity indexes of the reagents involved in these aryne-ene reactions were analysed.

DFT Study of the Inter-AE Reactions of Benzyne with Alkenes 7, 9 and 11 as well as the Intra-AE Reaction of Aryne 13

The analysis of the reaction paths associated with the AE reactions given in Scheme 7 indicates that the two chemical processes involved in these reactions, namely, the C–C single bond formation and the hydrogen transfer, occur in only one elementary step. Consequently, the reagents, one TS and the corresponding ene adduct for each of the four AE reactions were located and characterised (see Scheme 7). The relative electronic energies involved in these ene reactions are shown in Table 1, and the total electronic energies are given in the Supporting Information.

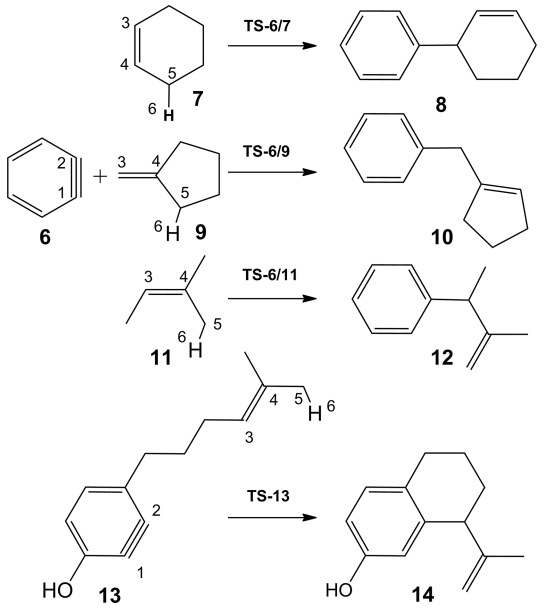

Scheme 7. Studied inter-AE reactions of **6** and intra-AE reaction of aryne **13**.

Table 1. MPWB1K/6-311G(d,p) relative electronic energies [kcal/mol] in the gas phase and in solution (in acetonitrile for inter-AE reactions and in THF for intra-AE reaction).

		Gas phase	Solvent phase
Inter-AE reactions of **6**			
7	**TS-6/7**	5.2 (5.5)[a]	0.6
	8	–94.5 (–94.1)[a]	–94.0
9	**TS-6/9**	–0.1	–0.5
	10	–97.7	–96.8
11	**TS-6/11**	1.2 (1.4)[b]	0.5
	12	–91.5 (–86.5)[b]	–90.0
Inter-AE reactions of **21**			
7	**TS-21/7**	4.1	–0.3
	22	–95.7	–95.3
9	**TS-21/9**	–0.8	–1.2
	23	–98.7	–98.1
Intra-AE reaction of **13**			
	TS-13	–0.3 (0.1)[a]	0.8
	14	–87.9 (–87.2)[a]	–87.7

[a] Gas-phase MPWB1K/6-311++G(d,p) optimisations. [b] Gas-phase CCSD(T)/6-311G(d,p) single-point energy calculations.

The activation energies associated with the inter-AE reactions of **6** with **7**, **9** and **11** in acetonitrile are 0.6 (**TS-6/7**), –0.5 (**TS-6/9**) and 0.5 kcal/mol (**TS-6/11**), and the reactions are strongly exothermic by 94.0 (**8**), 96.8 (**10**) and 90.0 kcal/mol (**12**). Two interesting conclusions can be obtained from these energy results: (1) These inter-AE reactions have insignificant activation energies. Note, that the energy of **TS-6/9** is even located below that of the reagents. (2) These reactions are strongly exothermic. The energy results indicate that **6** shows a very high reactivity, both kinetically and thermodynamically. Note that the polar ene reaction of isobutene with trifluoroacetaldehyde, an enophile with a similar electrophilicity ω index to that of **6**, presents an activation energy of 17.1 kcal/mol and is exothermic by 21.0 kcal/mol.[7]

To analyse the role of diffuse functions in the study of these ene reactions, the gas-phase stationary points involved in the inter-AE reaction between **6** and **7**, which corresponds to a more polar ene reaction (see later), and in the intra-AE reaction of aryne **13** were optimised at the MPWB1K/6-311++G(d,p) level. As shown in Table 1, the inclusion of diffuse functions modifies neither the kinetics nor the thermodynamics of the reaction. Both activation and reaction energies remain practically unchanged.

The high reactivity of **6** is associated with the 1,2-pseudodiradical vinyl character of the C1–C2 bonding region (see later). To test the feasibility of the MPWB1K functional to describe such character for benzyne, CCSD(T)/6-311G(d,p) single-point energy calculations of the gas-phase stationary points involved in the inter-AE reaction of **6** with **11** were performed. At this level of theory, the gas-phase activation energy is 1.4 kcal/mol, and the reaction is strongly exothermic by 86.5 kcal/mol (see Table 1). Consequently, although both computational approaches give the same kinetics, MPWB1K calculations yield a slightly more exothermic reaction. In any case, both models account for the high reactivity of benzyne associated with its pseudodiradical character.

In the same way, the intra-AE reaction of aryne **13** (see Scheme 4) in THF presents an unappreciable activation energy of 0.8 kcal/mol (**TS-13**) and the reaction is exothermic by 87.7 kcal/mol (**14**).

Lautens et al.[5] also examined the inter-AE reactions of 4,5-dimethylbenzyne (**20**) and the 1,3-benzodioxole derivative **21** with alkenes **7** and **9**, for which they found a similar reactivity to that of benzyne (see Scheme 8).

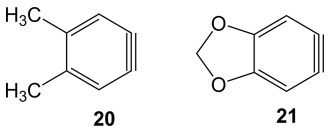

Scheme 8.

We also studied the inter-AE reactions of 1,3-benzodioxole derivative **21** with alkenes **7** and **9** (see Scheme 9). The corresponding activation and reaction energies are given in Table 1. The DFT calculations suggest that the 1,3-benzodioxole derivative **21** is slightly more reactive than benzyne **6**. In acetonitrile, the energies of both **TS-21/7** and **TS-21/9** are located below those of the reagents (see Table 1).

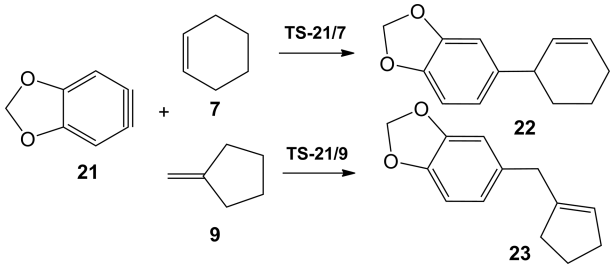

Scheme 9.

The relative enthalpies, entropies and Gibbs free energies of the stationary points involved in the inter-AE reactions of **6** with alkenes **7**, **9** and **11** as well as those of the intra-AE reaction of aryne **13** are given in Table 2. The enthalpies, entropies and Gibbs free energies of the stationary points are given in Table S4 in Supporting Information. The addition of the thermal corrections to the electronic energies increases the activation and reaction enthalpies by 1–4 kcal/mol. Consequently, the activation enthalpies have negligible changes, and all AE reactions are strongly exothermic. The addition of the entropies to the enthalpies has a different behaviour for the intra- and the inter-AE reactions. Although the activation and reaction Gibbs free energies for the intra-AE reaction of aryne **13** increase by 4–5 kcal/mol, those for the inter-AE reactions of benzyne increase by 11–15 kcal/mol owing to the unfavourable entropy associated with these bimolecular processes. In spite of the unfavourable entropic factor, the activation Gibbs free energies of the inter-AE reactions remain below 14 kcal/mol, an energy easily accessible at room temperature. On the other hand, the strong exergonic character of these AE reactions, below –74 kcal/mol, makes both the inter-AE and inter-AE reactions irreversible.

Table 2. MPW1K/6-311G(d,p) relative enthalpies ΔH [kcal/mol], entropies ΔS [cal/mol K] and Gibbs free energies ΔG [kcal/mol] of the stationary structures involved in the inter-AE reactions of **6** with alkenes **7**, **9** and **11** in acetonitrile and the intra-AE reaction of aryne **13** in THF; computed at 25 °C and 1 atm.

	ΔH	ΔS	ΔG
TS-6/7	1.3	–41.4	13.6
8	–90.7	–44.3	–77.5
TS-6/9	0.0	–38.7	11.5
10	–93.9	–48.5	–79.5
TS-6/11	0.9	–42.9	13.7
12	–87.4	–46.5	–73.5
TS-13	–1.4	–13.8	2.7
14	–85.8	–16.5	–80.9

The geometries of the TSs associated with the inter- and intra-AE reactions are given in Figure 1. In the gas phase, the lengths of the C1–C3 forming bonds in the TSs vary in a narrow range from 2.303 Å for **TS-21/9** to 2.199 Å for **TS-21/7**. Although the lengths of the C5–H6 breaking

bonds range from 1.100 to 1.125 Å in these TSs, the lengths of the C2–H6 forming bonds vary in a wider range from 2.041 to 2.317 Å. A comparison of the lengths involved in the formation of the C1–C3 single bond and in the hydrogen transfer process indicates that all TSs are associated with asynchronous processes in which the C1–C3 bond formation is more advanced than the hydrogen transfer process.

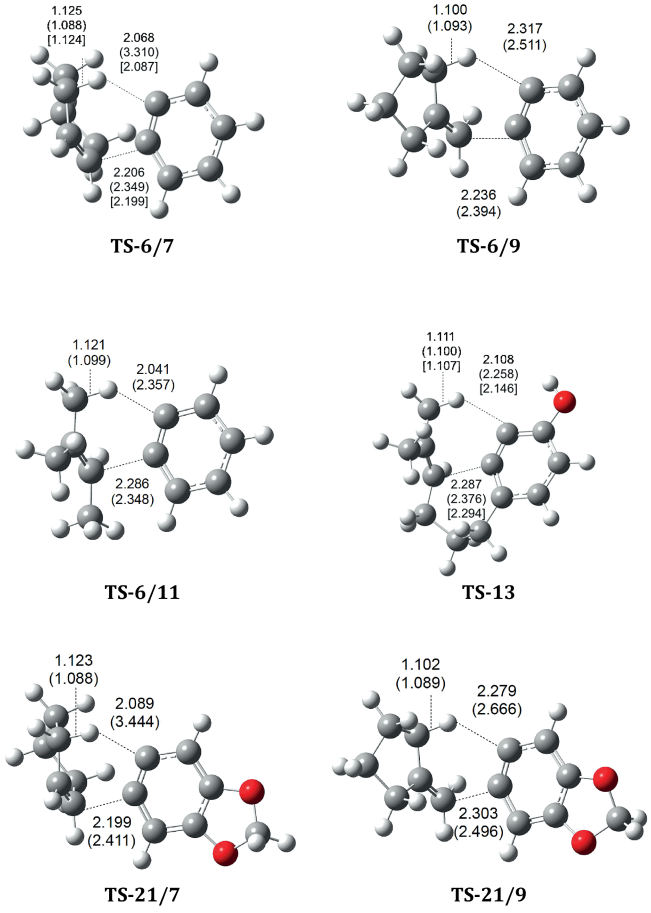

Figure 1. MPWB1K/6-311G(d,p) TS geometries associated with the AE reactions. The lengths [Å] are indicated, and the corresponding values in acetonitrile or THF are given in parentheses. The values corresponding to the MPWB1K/6-311++G(d,p) optimisations are given in brackets for **TS-6/7** and **TS-13**.

The bond lengths in acetonitrile or THF are shown in parentheses in Figure 1. The lengths of the C1–C3 forming bonds for the TSs in solutions are longer than those in the gas phase and range between 2.348 and 2.496 Å. On the other hand, the lengths of the C–H breaking bonds are slightly shorter than those in gas phase and range from 1.088 to 1.100 Å, and the lengths of the C–H forming bonds are longer and vary in the range 2.258 to 3.444 Å. Consequently, in acetonitrile or THF, the ene reactions are earlier. The geometrical parameters of the intermolecular **TS-6/11** and the intramolecular **TS-13** are very similar, and this resemblance indicates a similar bond evolution (see later). A comparison of these geometrical parameters for the TSs of the six AE reactions indicates that more favourable ene reactions proceed through more asynchronous processes.

Finally, the incorporation of diffuse functions through the 6-311++G(d,p) basis set does not produce significant changes in the geometrical parameters relative to those obtained at the 6-311G(d,p) level (see **TS-6/7** and **TS-13** in Figure 1). Consequently, no significant changes to the energies or geometries are observed with the inclusion of diffuse functions in the study of these ene reactions.

The polar nature of these AE reactions was analysed by computing the GEDT at the TSs. The natural atomic charges at the TSs, obtained through a natural population analysis (NPA), were shared between the aryne framework and that of the ene component. The atomic charges at the hydrogen atom that will be transferred are assigned to the ene framework. The values of the GEDT that flows from the ene component to the aryne are 0.23 e (**TS-6/7**), 0.21 e (**TS-6/9**), 0.21 e (**TS-6/11**), 0.11 e (**TS-13**), 0.25 e (**TS-21/7**) and 0.19 e (**TS-21/9**). In general, the GEDT range of 0.19 to 0.25 e allows these reactions to be classified in the borderline of N-ene and P-ene reactions.[7] Only the intra molecular **TS-13** presents a low GEDT value of 0.11 e and is classified as an N-ene reaction.

ELF Topological Analysis of Bonding Changes Along the Inter-AE Reaction between 6 and 16 as well as the Intra-AE Reaction of Aryne 13 – a Topological Characterisation of the C–C Bond Formation and the Hydrogen Transfer Process

A great deal of work has emphasised that the ELF topological analysis along a reaction path can be used as a valuable tool to understand the bonding changes and, thus, to establish the molecular mechanisms of reactions.[27] Several ELF topological analyses of organic reactions involving the C–C bond formation between C=X (X = C, N or O) double bonds have shown that the C–C single bond formation begins in the short C*x*–C*y* distance range of 1.9–2.0 Å by merging two monosynaptic basins, V(C*x*) and V(C*y*), into a new disynaptic basin V(C*x*,C*y*) associated with the formation of the new C*x*–C*y* single bond.[28] This behaviour indicates that C–C bond formation in these systems occurs through a C–C pseudodiradical[29] coupling between the two interacting centres of the reagents, which have some nonbonding electron density.[28]

Recently, the bonding changes along the N-ene and P-ene reactions have been topologically studied to understand the C–C bond formation and the hydrogen transfer process in ene reactions involving C=C and C=O enophiles.[7] Although the C–C bond formation and the hydrogen transfer processes are near synchronous in N-ene reactions, both processes are nonconcerted in P-ene reactions; the hydrogen transfer process only begins after the formation of the new C–C single bond. Interestingly, the formation of the new C–C single bond topologically begins at C–C distances of 2.02 Å in N-ene reactions and 1.96 Å in P-ene reactions.

To understand the C–C bond formation and the hydrogen transfer process in AE reactions, ELF topological

analyses of the MPWB1K/6-311G(d,p) wave functions of some relevant points of the IRCs of the model inter-AE reaction between **6** and **16** to yield adduct **30** and the intra-AE reaction of aryne **13** (see Scheme 4) were performed to characterise the molecular mechanisms of these AE reactions. Details of the ELF topological analysis are given in the Supporting Information.

From this ELF topological analysis, some interesting conclusions can be drawn: (1) The ELF topological analysis of the electronic structure of **6** indicates that the C1–C2 bonding region presents a 1,2-pseudodiradical vinyl structure rather than a C≡C triple bond one. As in the simplest azomethyne ylide (AY) **26** (CH_2–NH–CH_2),[29] this behaviour makes these species very reactive as they do not require the C–C or C–N bonds to be broken at the beginning of the reaction (see later). (2) In both inter- and intra-AE reactions, the corresponding TSs appear at very similar C1–C3 lengths: 2.387 Å for **TS-6/16** and 2.365 Å for **TS-13**. The unique remarkable topological changes observed at these TSs is the merger of two disynaptic basins associated with the C3–C4 double bond present in the enophile framework into only one V(C3,C4) disynaptic basin. (3) At a C1–C3 length of 2.07 Å, the C1 and C3 pseudoradical centres involved in the formation of the new C1–C3 single bonds are already created. (4) At a C1–C3 length of 1.92 Å, the two V(C1) and V(C3) monosynaptic basin are merged into a new V(C1,C3) disynaptic basin with initial electronic populations of 1.33 e (inter-AE) and 1.45 e (intra-AE). The creation of the V(C1,C3) disynaptic basin is associated with the formation of the new C1–C3 single bond in these AE reactions.[28] Although the C5–H6 single bond is not completely broken at this phase of the inter-AE reaction, the intra-AE one is already broken. Consequently, the formation of the C–C single bond and the hydrogen transfer process in these AE reactions are nearly synchronous. (5) For the hydrogen transfer process associated with these AE reactions, the presence of one V(H6) monosynaptic basin with a population of 1.25 e (inter-AE) and 0.89 e (intra-AE) indicates that a hydrogen atom is transferred in a nonpolar process.

The present ELF topological analyses along the IRCs of both inter- and intra-AE reactions indicate that the bonding changes occur in a nonconcerted fashion. The sequence of the bonding changes can be presented as (1) the formation of the pseudoradical centres at C1 and C3, (2) the formation of the new C1–C3 single bond and the hydrogen transfer process from C5 to C2, almost simultaneously, and (3) the formation of the new C4–C5 double bond in the ene adduct. Consequently, although the formation of the new C1–C3 bond and the hydrogen transfer process are topologically near synchronous processes, the migration of the C–C double bond in the ene component is not coupled. Unlike the ene reactions of C=C and C=O enophiles, which are initialised by the C=C or C=O breaking bond, AE reactions do not require this step as they already present a pseudoradical structure. As for other organic reactions, the formation of the new C1–C3 single bond occurs at a distance of ca. 1.92 Å through the C–C coupling of two pseudodiradical centres formed at the two interacting carbon atoms in a previous stage of the reaction.[28] This ELF topological analysis indicates that the bonding changes during these AE reactions are similar to those found in N-ene reactions involving C=C enophiles.

DFT Reactivity Analysis of the Ground States of the Reagents Involved in the AE Reactions

The AE reactions were analysed through the reactivity indices defined within the conceptual DFT.[30] The DFT reactivity indices, namely, the electronic chemical potential (μ), hardness (η), electrophilicity (ω) and nucleophilicity (N) of the reagents, are given in Table 3.

Table 3. MPWB1K/6-311G(d,p) electronic chemical potential (μ), hardness (η), electrophilicity (ω) and nucleophilicity (N) indices [eV] of the reagents. The reagents are ordered by decreasing ω values.

	μ	η	ω	N
Benzyne (**6**)	–4.65	7.31	1.48	2.10
1,3-Benzodioxole derivative **21**	–4.12	5.94	1.43	3.31
Aryne **13**	–4.11	6.03	1.40	3.27
4,5-Dimethylbenzyne (**20**)	–4.28	6.83	1.34	2.35
Methylenecyclopentane (**9**)	–3.27	9.64	0.55	2.31
2-Methyl-2-butene (**11**)	–3.08	9.34	0.51	2.65
Cyclohexene (**7**)	–2.97	9.23	0.48	2.82

The electronic chemical potentials μ of the ene components are between –3.27 (**9**) and –2.97 eV (**7**) and are higher than the those of the aryne species, which range from –4.11 (**13**) to –4.65 eV (**6**). Therefore, in the corresponding AE reactions, the GEDT goes from the ene components to the aryne ones, in clear agreement with the GEDT calculated at the TSs associated with the inter- and intra-AE reactions.

The electrophilicity ω index values of the arynes range from 1.34 (**20**) to 1.48 eV (**6**), and they are classified as moderate electrophiles. A comparison of the electrophilic ω index of these arynes with those of C=C and C=O enophiles indicates that these species could participate in P-ene reactions.[7] Although the nucleophilicity N indexes of **6** and the dimethyl derivative **20** (2.10 and 2.35 eV, respectively) classify them as moderate nucleophiles, the electron-rich arynes **13** and **21** have higher values (3.27 and 3.31 eV, respectively) and are classified as strong nucleophiles.

The ene components present very low electrophilicity ω indices (below 0.55 eV) and are classified as marginal electrophiles. The nucleophilicity N indices of these alkenes range from 2.31 (**9**) to 2.82 eV (**7**), and they are classified as moderate nucleophiles. Interestingly, the nucleophilicity N index of aryne **13** (3.27 eV), which has an unsaturated appendage, shows an N value higher than that of the enophile series.

As was mentioned in ref.[7] it may be stressed that the classification of ene reactions on the basis of the GEDT in the TSs into N-ene, P-ene and H-ene (i.e., nonpolar, polar and highly polar ene) reactions will depend on both the nucleophilic character of the ene component and the electrophilic character of the enophile. The analysis of the reac-

tivity indices and the GEDT at the corresponding TSs allows the classification of these AE reactions at the borderline of N-ene and P-ene reactions.[7] However, the activation energies of the ene reactions in ref.[7] are above 20 kcal/mol, which is very high compared with those of these AE reactions (below 5.0 kcal/mol). These results indicate that arynes present a particular behaviour that markedly enhances both kinetics and thermodynamics.

Benzyne can be represented by the four Lewis structures in Scheme 10.

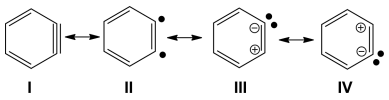

Scheme 10.

Lewis structure **I** represents the alkyne structure with a C≡C triple bond. On the other hand, structure **II** corresponds to a diradical structure, and structures **III** and **IV** correspond to zwitterionic structures. It is expected that structures **II**–**IV** will be less energetically favourable but more reactive (Scheme 10).

Although the nonpolar Diels–Alder reaction of butadiene (**24**) with **2** presents a high activation energy of 24.8 kcal/mol,[31] the nonpolar [3+2] cycloaddition reaction of the simplest AY **26** with **2** presents a insignificant activation energy of 1.2 kcal/mol (see Scheme 11).[29] An ELF topological analysis of the electronic structure of the simplest AY **26** showed that it presents a pseudodiradical ground-state structure similar to that demanded for synchronous C–C bond formation.[29] Consequently, the high reactivity of the simplest AY **26** was attributed to its pseudodiradical character.

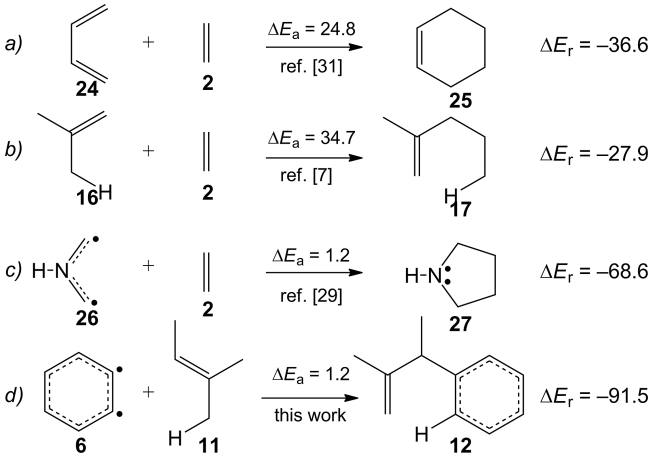

Scheme 11. Enhanced reactivity of pseudodiradical species **6** and AY **26**. The activation (ΔE_a) and reaction (ΔE_r) energies [kcal/mol] are indicated.

The ELF topological analysis of **6** (see Supporting Information) shows the presence of two nonbonding monosynaptic basins V(C1) and V(C2) at the C1 and C2 carbon atoms that integrate to 0.82 e each (see structure **6** in Scheme 11). This behaviour indicates that Lewis structure **II** (Scheme 10) will have a greater weight in the resonance structure of **6**; as for the simplest AY **26**,[29] this could explain the high reactivity of arynes when they are compared with that of **2**. Consequently, the 1,2-pseudodiradical vinyl structure rather than that with a C≡C triple bond is responsible for the very high reactivity of these species.

To ascertain that the high reactivity of arynes is due to the greater weight of structures **II**–**IV**, the isodesmic reaction given in Scheme 12 was considered.[32]

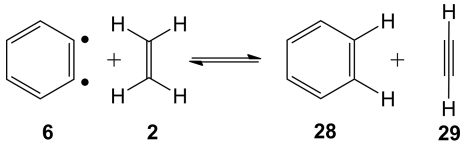

ΔE = –53.5 kcal/mol (MPWB1K/6-311G(d,p))
–48.8 kcal/mol (CCSD(T)/6-311G(d,p))

Scheme 12.

The isodesmic reaction given in Scheme 12 shows that **6** is ca. 54 kcal/mol thermodynamically more unstable than acetylene (**29**). This large destabilisation, which can be related to the unfeasibility of two sp-hybridised carbon atoms inside the six-membered carbocyclic system of **6**, is in reasonable agreement with the exothermic character of the ene reactions of **6** (–90 to –95 kcal/mol) when they are compared with the exothermic character of the ene reaction with **2** (–30 and –13 kcal/mol, see ref.[7]). Note that the [3+2] cycloaddition between the simplest AY **26**, which has a pseudodiradical structure, and ethylene **2** is also strongly exothermic (–68.6 kcal/mol, see Scheme 11).[29]

To validate the high instability of **6** attributed to its pseudodiradical character, single-point energy calculations at the CCSD(T)/6-311G(d,p) level were performed. The energy associated with the corresponding isodesmic reaction is given in Scheme 12. At this theoretical level, **6** is destabilised by ca. 49 kcal/mol with respect to acetylene (**29**). This thermodynamic data, which is similar to that for the reaction of **6** with **11** (see Table 1), reinforces the high reactivity shown by **6**. Finally, ELF topological analysis at the CCSD(T)/6-311G(d,p) level, with the Hartree–Fock-like formula for the ELF calculation by the CCSD(T) method, shows the presence of the two V(C1) and V(C2) monosynaptic basins associated with the two pseudoradical carbon atoms; therefore, the MPWB1K-DFT and CCSD(T) computational levels both provide a similar pseudodiradical structure (see Figure 2).

The kinetic and thermodynamic energy difference between reactions (b) and (d) in Scheme 11 can be related to the fact that the C–C double bond present in the ene reactions of alkenes must be broken to reach the pseudodiradical structures demanded for the C–C single bond formation. However, **6** does not require the previous C–C bond breaking bond as it has a resonant structure, as indicated by the Lewis structures shown in Scheme 10.

Recently, Yamabe et al.[33] and Zhao et al.[34] studied the cycloaddition reactions of **6** with tropone (**30**) and with carbon nanotubes, respectively, and found that these reactions proceed through stepwise mechanisms with diradical

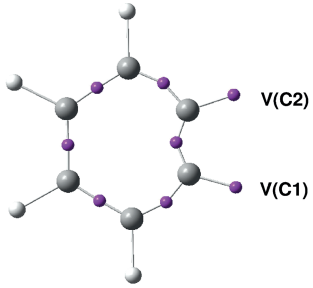

Figure 2. MPWB1K-DFT and CCSD(T) ELF attractors in **6**. The V(C1) and V(C2) monosynaptic basins are associated with the pseudoradical character of C1 and C2.

intermediates. Consequently, unrestricted calculations were demanded to analyse the mechanisms of these reactions. Interestingly, Yamabe et al. found that the activation energy associated with the formation of diradical intermediate **31** in the reaction of **6** with **30** (see Scheme 13) was 3.7 kcal/mol, a similar barrier to that found in the ene reaction between **6** and **7**.[33] Yamabe et al. conclude that "benzyne works as a diradical reagent along with as a dienophile toward conjugated compounds".[33] These findings are in complete agreement with the proposed pseudodiradical structure for **6**, which, depending on the counterpart reagent, can participate in closed-shell or open-shell mechanisms via diradical intermediates.

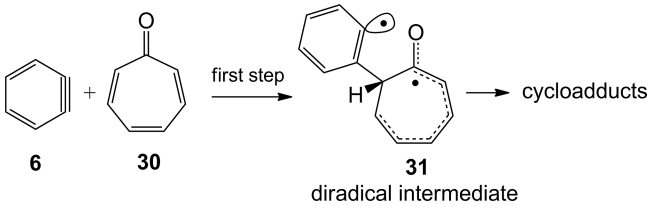

Scheme 13. Formation of diradical intermediate **31** in the reaction of **6** with **30**.[33]

Conclusions

The molecular mechanism of the inter- and intra-AE reactions has been theoretically studied by DFT methods at the MPWB1K/6-311G(d,p) level. These AE reactions occur through a one-step mechanism with nearly synchronous TSs in which the C–C single bond formation is slightly more advanced than the hydrogen transfer process. In all of the reactions, the arynes are very reactive. Thus, the activation energies of these AE reactions are less than 1 kcal/mol, and the reactions are strongly exothermic by more than 73 kcal/mol. Acetonitrile solvent slightly accelerates the inter-AE reactions, whereas THF slightly decelerates the intra-AE ones. For the geometry optimisations, the solvent increases the C–C distances at the TSs, and they occur earlier.

An ELF topological analysis of the bonding changes during the inter- and intra-AE reactions indicates the similarity of both reaction modes. As for the N-ene reaction of ethylenes, the ELF topological analysis indicates that the C–C bond formation and the hydrogen transfer processes are nearly synchronous. In addition, although the reactions begin with the breaking of the C–C double bond of the ene component, the formation of the new C–C double bond in the ene adducts occurs at the end of the reaction. Consequently, the bonding changes in these AE reactions are nonconcerted. As in other nonpolar and polar organic reactions featuring C=X (X = C, N, O) double bonds, the C–C single bond formation occurs at a distance of ca. 1.9 Å by a C–C coupling of two pseudoradical centres after the TS structures are passed.

Interestingly, although the GEDT at the TSs of the AE reactions (0.20–0.25 e) and the electrophilicity ω indexes of the arynes (1.34–1.48 eV) classify these reactions at the borderline of N-ene and P-ene reactions, they present a very high reactivity.

The ELF topological analysis of the electronic structure of benzyne indicates that it presents a pseudodiradical structure similar to that found in the simplest azomethyne ylide. Consequently, although the activation energy of the reaction for closed-shell enophiles can be related to the feasibility of the breaking of the C=C(X) double bonds present in the reagents to form the pseudoradical species involved in the C–C bond formation, the C–C bond formation occurs without any appreciable barrier for species with a pseudodiradical structure such as benzyne and the simplest azomethyne ylide. We can conclude that the 1,2-pseudodiradical vinyl structure of arynes rather than those with a C≡C triple bond are responsible for the very high reactivity of these species.

Supporting Information (see footnote on the first page of this article): ELF topological analysis of bonding changes during the intermolecular aryne-ene reaction between **6** and **16** as well as during the intramolecular aryne-ene reaction of aryne **13**; MPWB1K/6-311G(d,p) total electronic energies, enthalpies, entropies, and Gibbs free energies of the stationary points involved in the inter- and intramolecular aryne-ene reactions discussed in this work; MPWB1K/6-311G(d,p) gas-phase computed total energies, unique imaginary frequency, and Cartesian coordinates of the structures involved in the aryne-ene reactions.

Acknowledgments

This work has been supported by the Spanish Ministerio de Ciencia e Innovación (MICINN), project CTQ2013-45646-P, by the Universidad de Valencia, project UV-INV-AE13-139082, by the Fondo Nacional de Desarrollo Científico y Tecnológico (FONDECYT), grant number 1140341, and by the Millennium Nucleus of Chemical Processes and Catalysis (CPC), project number 120082. L. R. D. also thanks FONDECYT for continuous support through Cooperación Internacional.

[1] K. Mikami, M. Shimizu, *Chem. Rev.* **1992**, *92*, 1021–1050.
[2] a) J. Park, M. Yan, *Acc. Chem. Res.* **2013**, *46*, 181–189; b) A. Bhunia, S. R. Yetra, A. T. Biju, *Chem. Soc. Rev.* **2012**, *41*, 3140–3152; c) A. T. Biju, N. Kuhl, F. Glorius, *Acc. Chem. Res.* **2011**, *44*, 1182–1195; d) D. Peña, D. Pérez, E. Guitián, *Heterocycles* **2007**, *74*, 89–100; e) A. M. Dyke, A. J. Hester, G. C. Lloyd-Jones, *Synthesis* **2006**, 4093–4112.

[3] a) P. M. Tadross, B. M. Stoltz, *Chem. Rev.* **2012**, *112*, 3550–3577; b) H. Yoshida, K. Takaki, *Heterocycles* **2012**, *85*, 1333; c) T. Zhang, X. Huang, L. Wu, *Eur. J. Org. Chem.* **2012**, 3507–3519; d) C. M. Gampe, E. M. Carreira, *Angew. Chem. Int. Ed.* **2012**, *51*, 3766–3778; *Angew. Chem.* **2012**, *124*, 3829; e) T. Gerfaud, L. Neuville, J. Zhu, *Angew. Chem. Int. Ed.* **2009**, *48*, 572–577; *Angew. Chem.* **2009**, *121*, 580.

[4] Y. Himeshima, T. Sonoda, H. Kobayashi, *Chem. Lett.* **1983**, 1211–1214.

[5] D. A. Candito, D. Dobrovolsky, M. Lautens, *J. Am. Chem. Soc.* **2012**, *134*, 15572–15580.

[6] Z. Chen, J. Liang, J. Yin, G.-A. Yu, S. H. Liu, *Tetrahedron Lett.* **2013**, *54*, 5785–5787.

[7] a) L. R. Domingo, M. J. Aurell, P. Pérez, *Org. Biomol. Chem.* **2014**, *12*, 7581–7590.

[8] L. R. Domingo, J. A. Sáez, *Org. Biomol. Chem.* **2009**, *7*, 3576–3583.

[9] a) A. Savin, A. D. Becke, J. Flad, R. Nesper, H. Preuss, H. G. Vonschnering, *Angew. Chem. Int. Ed. Engl.* **1991**, *30*, 409–412; *Angew. Chem.* **1991**, *103*, 421; b) B. Silvi, A. Savin, *Nature* **1994**, *371*, 683–686; c) A. Savin, B. Silvi, F. Colonna, *Can. J. Chem.* **1996**, *74*, 1088–196; d) A. Savin, R. Nesper, S. Wengert, T. F. Fassler, *Angew. Chem. Int. Ed. Engl.* **1997**, *36*, 1808–1832; *Angew. Chem.* **1997**, *109*, 1892; e) Y. Grin, A. Savin, B. Silvi, *The ELF Perspective of Chemical Bonding*, in: *The Chemical Bond: Fundamental Aspects of Chemical Bonding* (Eds.: G. Frenking, S. Shaik), Wiley-VCH, Weinheim, Germany, **2014**, p. 345.

[10] L. R. Domingo, J. A. Sáez, R. J. Zaragozá, M. Arnó, *J. Org. Chem.* **2008**, *73*, 8791–8799.

[11] a) A. D. Becke, *J. Chem. Phys.* **1993**, *98*, 5648–5652; b) C. Lee, W. Yang, R. G. Parr, *Phys. Rev. B* **1988**, *37*, 785–789.

[12] W. J. Hehre, L. Radom, P. v. R. Schleyer, J. A. Pople, *Ab Initio Molecular Orbital Theory*, Wiley, New York, **1986**.

[13] Y. Zhao, G. D. Truhlar, *J. Phys. Chem. A* **2004**, *108*, 6908–6918.

[14] a) H. B. Schlegel, *J. Comput. Chem.* **1982**, *3*, 214–218; b) H. B. Schlegel "Geometry Optimization on Potential Energy Surfaces", in: *Modern Electronic Structure Theory* (Ed.: D. R. Yarkony), World Scientific Publishing, Singapore, **1994**.

[15] K. Fukui, *J. Phys. Chem.* **1970**, *74*, 4161–4163.

[16] a) C. González, H. B. Schlegel, *J. Phys. Chem.* **1990**, *94*, 5523–5527; b) C. González, H. B. Schlegel, *J. Chem. Phys.* **1991**, *95*, 5853–5860.

[17] a) J. Tomasi, M. Persico, *Chem. Rev.* **1994**, *94*, 2027–2094; b) B. Y. Simkin, I. Sheikhet, *Quantum Chemical and Statistical Theory of Solutions – A Computational Approach*, Ellis Horwood, London, **1995**.

[18] a) E. Cances, B. Mennucci, J. Tomasi, *J. Chem. Phys.* **1997**, *107*, 3032–3041; b) M. Cossi, V. Barone, R. Cammi, J. Tomasi, *Chem. Phys. Lett.* **1996**, *255*, 327–335; c) V. Barone, M. Cossi, J. Tomasi, *J. Comput. Chem.* **1998**, *19*, 404–417.

[19] a) A. E. Reed, R. B. Weinstock, F. Weinhold, *J. Chem. Phys.* **1985**, *83*, 735–746; b) A. E. Reed, L. A. Curtiss, F. Weinhold, *Chem. Rev.* **1988**, *88*, 899–926.

[20] A. D. Becke, K. E. Edgecombe, *J. Chem. Phys.* **1990**, *92*, 5397–5403.

[21] S. Noury, X. Krokidis, F. Fuster, B. Silvi, *Comput. Chem.* **1999**, *23*, 597–604.

[22] M. J. Frisch, G. W. Trucks, H. B. Schlegel, G. E. Scuseria, M. A. Robb, J. R. Cheeseman, G. Scalmani, V. Barone, B. Mennucci, G. A. Petersson, H. Nakatsuji, M. Caricato, X. Li, H. P. Hratchian, A. F. Izmaylov, J. Bloino, G. Zheng, J. L. Sonnenberg, M. Hada, M. Ehara, K. Toyota, R. Fukuda, J. Hasegawa, M. Ishida, T. Nakajima, Y. Honda, O. Kitao, H. Nakai, T. Vreven, J. A. Montgomery Jr., J. E. Peralta, F. Ogliaro, M. Bearpark, J. J. Heyd, E. Brothers, K. N. Kudin, V. N. Staroverov, R. Kobayashi, J. Normand, K. Raghavachari, A. Rendell, J. C. Burant, S. S. Iyengar, J. Tomasi, M. Cossi, N. Rega, J. M. Millam, M. Klene, J. E. Knox, J. B. Cross, V. Bakken, C. Adamo, J. Jaramillo, R. Gomperts, R. E. Stratmann, O. Yazyev, A. J. Austin, R. Cammi, C. Pomelli, J. W. Ochterski, R. L. Martin, K. Morokuma, V. G. Zakrzewski, G. A. Voth, P. Salvador, J. J. Dannenberg, S. Dapprich, A. D. Daniels, O. Farkas, J. B. Foresman, J. V. Ortiz, J. Cioslowski, D. J. Fox, *Gaussian 09*, Gaussian, Inc., Wallingford CT, **2009**.

[23] a) R. G. Parr, L. Von Szentpaly, S. B. Liu, *J. Am. Chem. Soc.* **1999**, *121*, 1922–1924; b) P. K. Chattaraj, U. Sarkar, D. R. Roy, *Chem. Rev.* **2006**, *106*, 2065–2091.

[24] a) R. G. Parr, R. G. Pearson, *J. Am. Chem. Soc.* **1983**, *105*, 7512–7516; b) R. G. Parr, W. Yang, *Density Functional Theory of Atoms and Molecules*, Oxford University Press, New York, **1989**.

[25] a) L. R. Domingo, E. Chamorro, P. Pérez, *J. Org. Chem.* **2008**, *73*, 4615–4624; b) L. R. Domingo, P. Pérez, *Org. Biomol. Chem.* **2011**, *9*, 7168–7175.

[26] W. Kohn, L. Sham, *Phys. Rev. A* **1965**, *140*, 1133–1138.

[27] a) V. Polo, J. Andrés, S. Berski, L. R. Domingo, B. Silvi, *J. Phys. Chem. A* **2008**, *112*, 7128–7136; b) J. Andrés, S. Berski, L. R. Domingo, V. Polo, B. Silvi, *Curr. Org. Chem.* **2011**, *15*, 3566–3575; c) J. Andrés, P. González-Navarrete, V. S. Safont, *Int. J. Quantum Chem.* **2014**, *114*, 1239–1252.

[28] L. R. Domingo, *RSC Adv.* **2014**, *4*, 32415–32428.

[29] L. R. Domingo, E. Chamorro, P. Pérez, *Lett. Org. Chem.* **2010**, *7*, 432–439.

[30] a) P. Geerlings, F. De Proft, W. Langenaeker, *Chem. Rev.* **2003**, *103*, 1793–1874; b) D. H. Ess, G. O. Jones, K. N. Houk, *Adv. Synth. Catal.* **2006**, *348*, 2337–2361.

[31] E. Goldstein, B. Beno, K. N. Houk, *J. Am. Chem. Soc.* **1996**, *118*, 6036–6043.

[32] F. A. Carey, R. J. Sundberg, *Advanced Organic Chemistry Part A: Structure and Mechanisms*, Springer, New York, **2000**.

[33] S. Yamabe, T. Minato, T. Watanabe, T. Machiguchi, *Theor. Chem. Acc.* **2011**, *130*, 981–990.

[34] T. Yang, X. Zhao, S. Nagase, *Org. Lett.* **2013**, *15*, 5960–5963.

Received: December 9, 2014
Published Online: March 17, 2015

